

Available online at [www.sciencedirect.com](http://www.sciencedirect.com)

SciVerse ScienceDirect

<http://www.elsevier.com/locate/biombioe>

# Organic fractions influence on biogas generation from potato residues. Kinetic model generalization



Ignacio Durruty<sup>a,\*</sup>, Noemí E. Zaritzky<sup>b</sup>, Jorge Froilán González<sup>a</sup>

<sup>a</sup> Grupo de Ingeniería Bioquímica, Departamento de Ingeniería Química, Facultad de Ingeniería, UNMDP, Juan B. Justo 4302, 7600 Mar del Plata, Bs. Aires, Argentina

<sup>b</sup> Centro de Investigación y Desarrollo en Criotecología de Alimentos (CIDCA, UNLP-CONICET), and Facultad de Ingeniería UNLP, 47 y 116, B1900AJJ La Plata, Bs. Aires, Argentina

## ARTICLE INFO

### Article history:

Received 9 May 2013

Received in revised form

24 September 2013

Accepted 27 September 2013

Available online 17 October 2013

### Keywords:

Biomethane production

COD fraction

Kinetic

Inhibition

Fed fluctuation

## ABSTRACT

Bioenergy production as methane is being increasingly used to process low value by-products or not commercial wastes, in particular those which contain high levels of biodegradable organic matter such as potato residue. This work is a continuation of a previous one, which details the characterization and development of a kinetic model for its biodegradation. The knowledge of the effect of different fed organic fractions on the kinetics allows the development of kinetic models that predict the behavior of the degradation after a fluctuation in the feed characteristics. Information about the influence of each variable over different process stages was found and a generalized model was developed in concordance. It considers: substrate inhibition in the hydrolysis step and uncompetitive inhibition by total organic load in the stage of degradation of the biodegradable soluble material, and the yield of methane. Furthermore, the biomass influence was taken into account on each stage. This generalized model has been successfully able to predict the evolution of the different species throughout the whole range of conditions studied with a single set of parameters.

© 2013 Elsevier Ltd. All rights reserved.

## 1. Introduction

During anaerobic digestion the organic material is biologically converted to a variety of end products including biogas, whose main components are methane (65–70%) and carbon dioxide (25–35%) [1,2]. Thus, the anaerobic digestion presents the advantages of treating influents with high organic concentrations coupled with bioenergy recovery [3]. Furthermore, the high values of chemical energy available in potato starch made the potato residue suitable for energy production by anaerobic digestion [4]. Besides, the use of a residue as raw material to generate energy could presents economical

benefits. Also, a possible source of increased revenue available to industries is through taking advantage of the incentives awarded by the Clean Development Mechanism (CDM) under the Kyoto Protocol 1997. Finally, anaerobic digestion appears to be a promising technology to attain revenue from Certified Emission Reduction (CER) credits, more commonly known as carbon credits from the CDM as methane gas is generated and can be utilized as renewable energy [3].

Potato wastes contain both soluble and particulate organic load [5]. A sound kinetic modeling of the anaerobic degradation of complex substrates is increasingly needed for a better understanding of the performance of these systems [6]. A

\* Corresponding author. Biochemical Engineering Group, Engineering School, National University of Mar del Plata, Juan B. Justo 4302, CP. 7600 Mar del Plata, Argentina. Tel.: +54 223 481 6600x261; fax: +54 223 481 0046.

E-mail addresses: [durruty@fi.mdp.edu.ar](mailto:durruty@fi.mdp.edu.ar) (I. Durruty), [zaritzky@ing.unlp.edu.ar](mailto:zaritzky@ing.unlp.edu.ar) (N.E. Zaritzky), [froilan@fi.mdp.edu.ar](mailto:froilan@fi.mdp.edu.ar) (J.F. González). 0961-9534/\$ – see front matter © 2013 Elsevier Ltd. All rights reserved.

<http://dx.doi.org/10.1016/j.biombioe.2013.09.013>

Nomenclature	
COD	chemical oxygen demand expressed as mg of oxygen divided by liter of solution ( $\text{mg L}^{-1}$ )
$k_1$	specific kinetic coefficient for degradation of biodegradable particulate matter ( $\text{L mg}^{-1} \text{d}^{-1}$ )
$k_2$	specific kinetic coefficient for degradation of soluble particulate matter ( $\text{L mg}^{-1} \text{d}^{-1}$ )
$k_{\text{max}_1}$	maximum specific rate constant for $r_1$ (generalized model) ( $\text{mg L}^{-1} \text{d}^{-1}$ )
$k_{\text{max}_2}$	maximum specific rate constant for $r_2$ (generalized model) ( $\text{mg L}^{-1} \text{d}^{-1}$ )
$K_{I1}$	inhibition constant for $r_1$ (generalized model) ( $\text{mg L}^{-1}$ )
$K_{I2}$	inhibition constant for $r_2$ (generalized model) ( $\text{mg L}^{-1}$ )
$K_{IM}$	inhibition constant for $Y_{M/SB}$ (generalized model) ( $\text{mg L}^{-1}$ )
$K_{S1}$	half life constant for $r_1$ ( $\text{mg L}^{-1}$ )
$M$	methane volume per unit of reaction volume expressed as equivalent COD ( $\text{mg L}^{-1}$ )
$m$	biomass maintenance coefficient for $Y_{M/SB}$ (generalized model) ( $\text{L mg}^{-1}$ )
$n$	order which affects $x_{XP}$ in $r_2$ (generalized model)
$r_2$	degradation rate of $X_B$ ( $\text{mg L}^{-1} \text{d}^{-1}$ )
$r_2$	net degradation rate of $S_B$ ( $\text{mg L}^{-1} \text{d}^{-1}$ )
$r_M$	methane production rate ( $\text{mg L}^{-1} \text{d}^{-1}$ )
$r_P$	biomass production rate ( $\text{mg L}^{-1} \text{d}^{-1}$ )
$S_B$	soluble biodegradable COD fraction ( $\text{mg L}^{-1}$ )
$S_I$	soluble inert COD fraction ( $\text{mg L}^{-1}$ )
$S_P$	soluble metabolic product COD fraction ( $\text{mg L}^{-1}$ )
SCOD	soluble chemical oxygen demand ( $\text{mg L}^{-1}$ )
$t$	time (d)
TCOD	total chemical oxygen demand ( $\text{mg L}^{-1}$ )
$x_{SB}$	ratio between initial biodegradable soluble fraction and the initial total organic load
$x_{SI}$	ratio between inert soluble fraction and the initial total organic load
$x_{xB}$	ratio between initial biodegradable particulate fraction and the initial total organic load
$x_{xI}$	ratio between inert particulate fraction and the initial total organic load.
$x_{xP}$	ratio between initial particulate product (inoculum) and the initial total organic load
$X_B$	particulate biodegradable COD fraction ( $\text{mg L}^{-1}$ )
$X_I$	particulate inert COD fraction ( $\text{mg L}^{-1}$ )
$X_P$	particulate product COD fraction, biomass ( $\text{mg L}^{-1}$ )
$Y$	global methane yield coefficient ( $\text{L}_{\text{CH}_4} \text{g}^{-1}$ )
$Y_H$	particulate biodegradable to soluble biodegradable yield coefficient or hydrolysis yield coefficient
$Y_{M/xB}$	global yield coefficient that represents the contribution on methane production of particulate degradation.
$Y_{M/SB}$	global yield coefficient that represents the contribution on methane production of soluble biodegradable degradation.
$Y_{\text{max}_M}$	maximum yield coefficient (generalized model)
$Y_{SP/SB}$	soluble biodegradable matter to soluble metabolic products yield coefficient
$Y_{XP/SB}$	soluble biodegradable matter to particulate products yield coefficient

major prerequisite for modeling is a reliable fed characterization. This can be achieved with a proper discrimination of the Chemical Oxygen Demand (COD) loads with different biodegradability characteristics. In a previous work Durruty et al. [7] presented a method to characterize the different organic fractions based on a modification of the Orhon method [8]. With this tool, the fractions of biodegradable and inert COD load can be also separated into both soluble and particulate fraction. This discrimination method can be used to evaluate the effect of each organic fraction on the kinetics of degradation.

The presence of particulate matter and its concentration has been shown to influence the kinetics of the degradation process and methane generation [9–11]. However, Parawira et al. [12] highlighted the lack of information on the influence of different operating parameters such as total solid and inoculum substrate ratio on these processes for certain substrates, among which potato wastes are included. Furthermore, research on the effect of organic load or the organic load-inoculum ratio [12–17] has demonstrated that these factors may be efficient tools to improve the process without the addition of any easy-degradable carbon source. Additionally, knowledge of the impact of the organic load on the treatment allows the development of kinetic models that predict the behavior after a fluctuation in the feed flow. This is

considered relevant, since the stability against changes in reactor inlet is one of the most important considerations for the design of this kind of process [18].

Kinetic models, whose parameters must be set for each initial condition, have been previously reported in literature [10,19]. These models are useful to study and compare the performance of the process based on the composition. However, they are not so useful in those applications where inlet conditions may vary considerably. Such variability is very common where low value byproducts or residues are used as substrates for energy generation. In the particular case of potato waste its composition depends strongly of variations of the industrial plant operation and the market value of potato starch. Thus, it is very important to develop models that take into account the effect of the feed on the performance of the process, without becoming extremely complex such as the ADM1 model [20]. Inhibitory kinetic models such as the Andrews–Haldane models, Yano, Webbs, Teissier Aiba, etc [21,22] generally have global orders different than one or present exponential relationships. Examples of these models applied to anaerobic systems are found in literature for substrate inhibition [23,24], external inhibitors [23,25] or related to biomass [26].

With the aim to improve the knowledge on bioenergy production as methane, this work introduces a model able to

allow not only prediction of the behavior after a fluctuation in the feeding, but also a preliminary reactor design and process optimization. Thus, the objectives were: a) to study the effects of different organic loads over the energy generation performance; b) to improve the previously presented kinetic model making it able to predict the anaerobic digestion of potato waste under a wide range of feeding conditions.

### 1.1. Previous kinetic model

In particular, potato waste contain particulate and soluble organic load, mainly in the form of starch and soluble carbohydrates, which are assimilated by anaerobic microorganisms at different rates. As described in Durruty et al. [7] the total COD can be divided into a refractory or inert (I) organic fraction and a biodegradable (B) organic fraction. Both fractions, the inert and the biodegradable, can in turn be split into soluble (S) and particulate (X) fractions. Fig. 1 outlines the kinetic model based on this COD fractionation. It is assumed that the particulate biodegradable matter ( $X_B$ ) is degraded to soluble biodegradable matter ( $S_B$ ) and acetate that is not detectable by COD method [27]. It can be assumed that the acetate produced during hydrolysis is directly converted to methane (M) by acetoclastic methanogenic bacteria [2]. Later, the kinetic model assumes that the metabolic products ( $S_P$ ), biomass ( $X_P$ ) and methane (M) are produced during the soluble biodegradable matter ( $S_B$ ) degradation [7].

Thus, a specific first order serial–parallel reactions kinetic model can be used to describe the kinetic behavior. Taking into account the reaction scheme shown in Fig. 1, the particulate biodegradable organic fraction degradation of  $X_B$  ( $r_1$ ) and the net degradation rate of  $S_B$  ( $r_2$ ) are given by:

$$\frac{dX_B}{dt} = (r_1) = -k_1 \cdot X_p \cdot X_B \quad (1)$$

$$\frac{dS_B}{dt} = (r_2) = Y_H \cdot k_1 \cdot X_p \cdot X_B - k_2 \cdot X_p \cdot S_B \quad (2)$$

The biomass production ( $r_p$ ) can be represented by:

$$\frac{dX_p}{dt} = (r_p) = Y_{XP/SB} \cdot k_2 \cdot X_p \cdot S_B \quad (3)$$

Analogously,  $S_P$  and M production rate ( $r_M$ ) can be described as follows:

$$\frac{dS_P}{dt} = Y_{SP/SB} \cdot k_2 \cdot X_p \cdot S_B \quad (4)$$

$$\frac{dM}{dt} = (r_M) = Y_{M/XB} \cdot k_1 \cdot X_p \cdot X_B + Y_{M/SB} \cdot k_2 \cdot X_p \cdot S_B \quad (5)$$

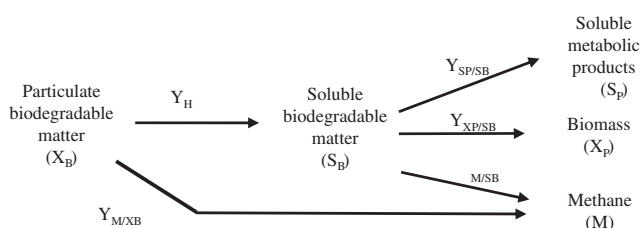


Fig. 1 – Kinetic reaction scheme.

## 2. Materials and methods

### 2.1. Substrate and inoculum

The substrate for anaerobic digestion used was a simulated potato residue. It was prepared by grinding whole fresh potatoes and adding distilled water in a ratio of 1 L of water to 100 g of fresh potatoes. The resulting suspension was filtered by vacuum through a sieve (mesh size 20  $\mu\text{m}$ ). The addition of water took place in successive leaching stages and washing of cake. Finally peptone was added to ensure the nutrient requirement of COD/N/P ratio 200/5/1. Anaerobic sludge from a working methanogenic industrial digester was used as inoculum. It was kindly supplied by McKein SA (Balcarce, Argentina), from its anaerobic wastewater treatment plant.

### 2.2. Analytical methods

The COD was determined using method 5520 (Closed Reflux Method) [27]. Samples of 2 ml each were centrifuged for 10 min at 9000 G. 1 ml of supernatant was taken for determination of soluble COD. The total COD was measured using non-centrifuged samples after being homogenized in a Wheaton homogenizer and then diluted in distilled water.

### 2.3. Experimental procedure

Four batch experiments (I, II, III and IV depicted in Table 1) were conducted at least by duplicate, in a 1.5 L anaerobic reactor with temperature control (35  $^{\circ}\text{C}$ ) and agitation (4  $\text{s}^{-1}$ ). The initial ratio SCOD/TCOD and the total organic load (TCOD) of experiments I, II, III and IV were selected to study the effects of the ratio of soluble/solid organic fractions over the degradation and they are shown on Table 1. Different organic fractions ( $X_I$ ,  $X_B$ ,  $X_P$ ,  $S_I$ ,  $S_B$ ) and initial percentages ( $x_{xI}$ ,  $x_{xB}$ ,  $x_{xP}$ ,  $x_{sI}$ ,  $x_{sB}$ ) were calculated by the method previously developed by Durruty et al. [7]. The pH was adjusted to 7.2 thorough all the experiments using phosphate-buffer. During the batch tests, samples were taken at regular intervals to monitor pH and composition.

### 2.4. Kinetic parameter and statistical analysis

The kinetic coefficients  $k_1$  and  $k_2$  were obtained by fitting the data of the organic fractions  $X_B$  and  $S_B$ , versus time by the least squares method (Origin 8.0, Originlab corporation). The yield coefficients  $Y_H$ ,  $Y_{XP/SB}$ ,  $Y_{SP/SB}$ ,  $Y_{M/XB}$  and  $Y_{M/SB}$  were calculated according to the procedure described by Durruty et al. [7]. Furthermore, a parameter Y is defined here as the global methane yield coefficient. The parameters obtained independently for each case are shown in Table 2. The linear regressions and “forward” statistical analysis were performed with R v2.12. (R project). Once the kinetic parameters were obtained, the concentration profile was modeled using a fourth-order Runge–Kutta algorithm coupled to the regression in order to integrate the equations simultaneously (MathCad 14.0.0.163, Parametric Technology Corporation).

**Table 1 – Initial wastewater composition in different batch assays.**

Exp	TCOD	SCOD	$X_B$	$X_I$	$S_B$	$S_I$	$X_P$	$X_{XB}$	$X_{XI}$	$X_{SB}$	$X_{SI}$	$X_{XP}$
			mg L <sup>-1</sup>									
I	2636	2220	18	33	1958	262	364	0.7	1.2	74.3	10.0	14.0
II	4457	3023	1056	68	2832	190	310	23.7	1.6	63.5	4.3	7.0
III	6517	4473	1502	0	4335	138	542	25.1	0.0	72.6	2.2	8.3
IV	6810	2876	3427	47	2569	307	460	50.3	0.6	37.7	4.5	6.8

### 3. Results and discussion

Table 2 shows the kinetic parameters  $k_1$  and  $k_2$  together with  $Y_{M/xB}$ ,  $Y_{M/SB}$  and  $Y$  yield coefficients, obtained by independently fitting the model developed by Durruty et al. [7] to the results from the experiments I, II, III and IV. Looking at the data, an inverse relationship can be seen between the organic load and the kinetic constants, what agrees with the results of to Siles et al. [10]. The values of  $k_1$  and  $k_2$  are within the range reported in literature [9,11,17]. In a similar way, the value of the methane yield coefficient obtained falls among those previously reported [28] and lies below the maximum reported by McCarty [29]. The experimental and predicted values are shown as dashed lines on Figs. 2–5 for the experiments I, II, III and IV respectively. In these figures it can be observed how the model developed by Durruty et al. [7] predicts properly the experimental performance. However, it shows better predictions in the early stages of the degradation. This phenomenon is most evident in the experiments with higher initial organic load (III, IV) in which the predicted  $S_B$  overestimates the experimental values towards: in the last stages of the degradation and some uncertainty was observed at intermediate times.

#### 3.1. Linear correlations

Table 3 shows the linear correlations between different organic fractions. The high value of the regression coefficient indicates a strong correlation between TCOD,  $X_{B(t=0)}$  and  $S_{I(t=0)}$  and between  $x_{XI}$  and  $x_{XP}$ . On the other hand there is a very low correlation between  $S_{B(t=0)}$  and TCOD and between SCOD,  $x_{XP}$  and  $X_{I(t=0)}$ .

Table 4 shows the linear correlations between organic fractions and the obtained parameters. A negative linear correlation higher than 0.9 for the kinetic constants  $k_1$  and  $k_2$  versus TCOD can be observed. This means that as the total organic load increases the kinetic constants decrease,

indicating an inhibitory effect at total organic loads higher than 2500 mg L<sup>-1</sup>. Results of this kind have not been reported on the anaerobic degradation of potato wastewater. Also, these results are consistent with results previously reported by Siles et al. [10] who observed inhibition by total organic load in the anaerobic degradation kinetics of orange residues for COD loads above 2000 mg L<sup>-1</sup> in all degradation stages. Also Fang and Yu [15] observed that the anaerobic degradation of gelatin wastewater was impaired by the increased concentration of the organic load at concentrations higher than 2000 mg L<sup>-1</sup>.

The observed values of  $Y_{M/xB}$  remained in the order of 0.1 for all the assays, so its linear relationship with the co-variables is not deemed to be relevant. Since  $Y$  includes  $Y_{M/xB}$  and  $Y_{M/SB}$ , the high correlation between  $Y_{M/SB}$  and  $Y$  ( $R > 0.98$ ) is not surprising since  $Y_{M/xB}$  can be considered constant. TCOD correlates very well with  $Y_{M/SB}$ . The sign of the correlation indicates a negative effect on the methane yield as the TCOD increases. This is consistent with previous reports on the anaerobic digestion of wastes from the potato industry with high organic loads [12,13].

Table 4 shows how  $k_1$  has a high linear correlation with  $X_B$  with negative sign, indicating substrate inhibition for the hydrolysis step and also with TCOD. However, the rate constant could have an independent correlation with both or, with only one variable and the effect should be translated to the other (due to the high correlation between TCOD and  $X_B$ ). For this reason the significance must be assessed in a multiple linear regression model. These linear models are widely used for parametric analysis datasets, in biological systems [30] and also in anaerobic digestion systems [31].

To evaluate the degree of mutual significance of the different co-variables in the multiple linear regression models, a “forward” procedure is usually carried out. This method consists on adding one at a time each independent variable to a multiple linear model, beginning with the most significant and evaluating the significance of each added variable in presence of the previously added. The most influential variable on  $k_1$  was  $X_B$  followed by TCOD with a low level of significance ( $P(F) > 0.23$  in both cases). However, once  $X_B$  was included in the model, TCOD lost significance, indicating that the original great significance over  $k_1$  could be attributed to its correlation with  $X_B$  ( $p$ -value: 0.2296  $R_{adjusted}$ : 0.7509).

When the influence over  $k_2$  was studied, the linear regression showed that the most significant variable was the percentage of initial inoculum ( $x_{XP}$ ) ( $P(F) = 0.02138$ ), analogous to the inoculum to substrate ratio (ISR) reported in literature [12,17]. As the inoculum-substrate ratio increases,  $k_2$  increase. Parawira et al. [12] found that, at 60% of initial inoculum, the

**Table 2 – Kinetic parameters and methane yield coefficients in different batch assays.**

Exp	$k_1$	$k_2$	$Y_{M/xB}$	$Y_{M/SB}$	$Y$
	L mg <sup>-1</sup> d <sup>-1</sup>				L <sub>CH4</sub> g <sup>-1</sup>
I	–	$2.395 \times 10^{-4}$	–	0.305	0.140
II	$1.77 \times 10^{-3}$	$1.008 \times 10^{-4}$	0.109	0.125	0.061
III	$1.01 \times 10^{-3}$	$0.9456 \times 10^{-4}$	0.096	0.085	0.052
IV	$0.29 \times 10^{-3}$	$0.6785 \times 10^{-4}$	0.125	0.015	0.043

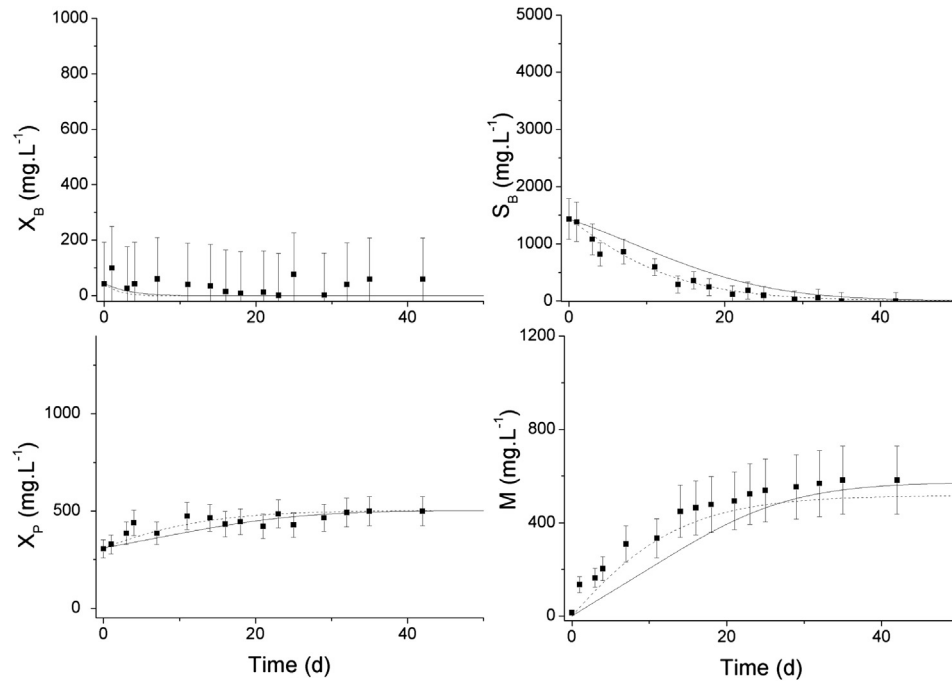


**Fig. 2 – Experimental values versus time for assay I. The dashed lines represent the theoretical values predicted by a previous model developed by Durruty et al. [7]. The solid lines represent the theoretical values predicted by the generalized model developed in this work.**

potato waste anaerobic degradation performance was optimal. The ratios worked within this work are well below that percentage, so it is expected that an increase in inoculum will result in an improvement in the development process. There is evidence in the literature that inhibition of a

biological process depends not only on the substrate concentration of the inhibitor but also on the relationship inoculum to substrate [32,33]. After inclusion of the variable  $x_{xp}$  in the model, the next most significant variable was TCOD ( $P(F) = 0.2464$ ) ( $p$ -value: 0.0079  $R_{adjusted}$ : 0.9998).

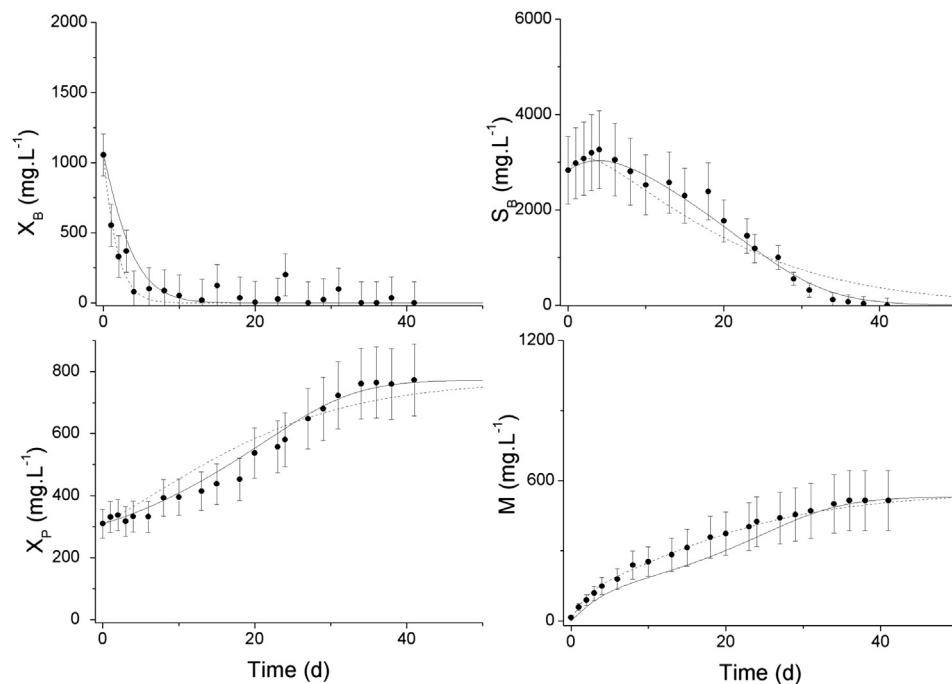


**Fig. 3 – Experimental values versus time for assay II. The dashed lines represent the theoretical values predicted by a previous model [7]. The solid lines represent the theoretical values predicted by the generalized model.**

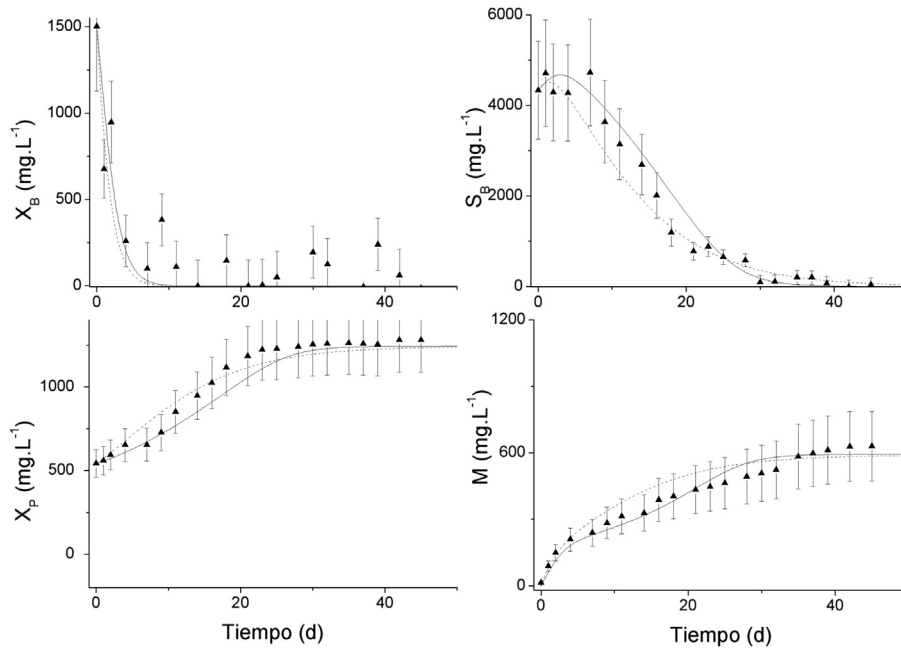


**Fig. 4 – Experimental values versus time for assay III. The dashed lines represent the theoretical values predicted by a previous model [7]. The solid lines represent the theoretical values predicted by the generalized model.**

In this work, the methane yield is highly correlated with the amount of initial inoculum  $X_P$ , which is the most significant variable after adding TCOD to the model ( $p$ -value: 0.0003  $R_{\text{adjusted}}$ : 0.9999). The variable  $x_{xB}$  is linearly significant; however by introducing TCOD in the model it lost significance, demonstrating that they are not mutually significant. More biomass generates higher maintenance requirements that

generally reduce the yield coefficients of both products and microbial growth [34]. In the case of anaerobic degradation experimental data have shown that the inoculum/substrate ratio affects both the rate and the yield [16]. The increase in methane yield due to the increase in the inoculum size is consistent with the results of Parawira et al. [12] for low percentages.

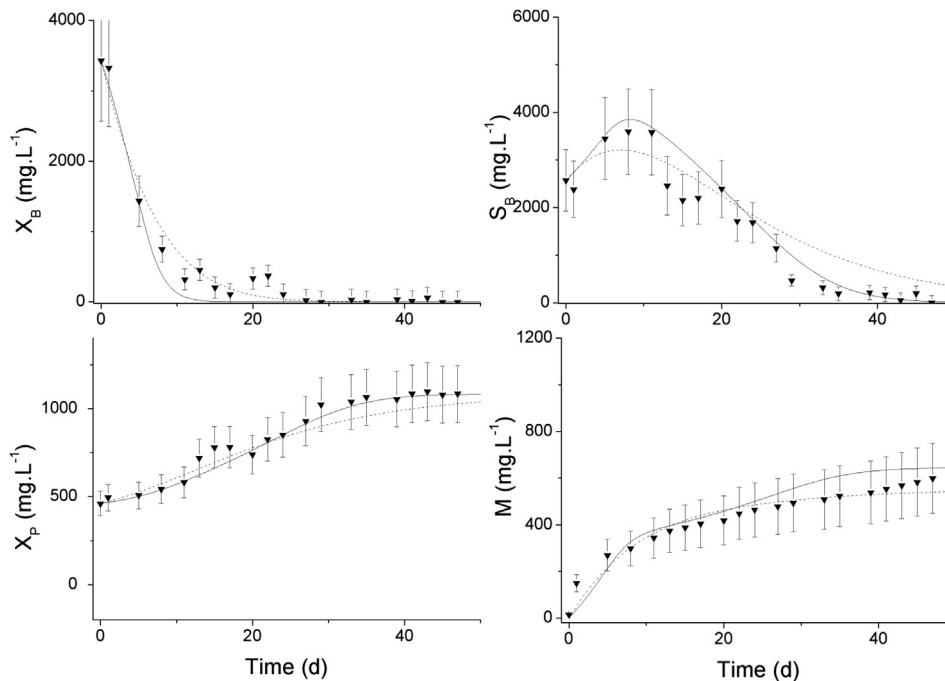


**Fig. 5 – Experimental values versus time for assay IV. The dashed lines represent the theoretical values predicted by a previous model [7]. The solid lines represent the theoretical values predicted by the generalized model.**

**Table 3 – Correlation matrix: organic fractions.**

	TCOD	SCOD	X <sub>B0</sub>	X <sub>I0</sub>	S <sub>B0</sub>	S <sub>I0</sub>	X <sub>P0</sub>
TCOD	1						
SCOD	0.88673	1					
X <sub>B0</sub>	0.98445	0.79237	1				
X <sub>I0</sub>	0.50503	0.17999	0.59859	1			
S <sub>B0</sub>	−0.10141	0.31624	−0.24360	−0.67173	1		
S <sub>I0</sub>	0.94016	0.77146	0.94272	0.62740	−0.35966	1	
X <sub>P0</sub>	−0.23462	0.01183	−0.30547	−0.86984	0.74748	−0.48956	1

### 3.2. Non-linear correlations

Table 5 shows the parameters and the correlation ( $R^2$ ) to an  $n$ -th order of different kinetic parameters versus the variables shown to be most significant linear correlations according to the equation:

$$P = A \cdot X^n \quad (6)$$

where  $P$  is the parameter and  $x$  the variable.

Table 5 shows that  $k_1$  has a much better fit versus  $X_B$  and presents an order of  $-1.5$ , which is similar to the global order of Haldane equation which is the most used substrate inhibition kinetic model [24,35]. In turn,  $k_2$  has a low correlation with  $S_B$  indicating absence of substrate inhibition at this stage. The order for  $k_2$  versus TCOD close to  $-1$  indicates an inhibition by this variable. Furthermore, the order for  $X_B$  is close to zero, what demonstrates independence of this parameter with this variable. While the high order regarding  $X_{XP}$  shows a high dependence from this variable.

$Y_{M/XB}$  did not correlate well with any of the different variables. Moreover, the correlation orders close to 0, indicate that  $Y_{M/XB}$  remains constant. Similarly,  $Y_{M/SB}$  did not show a good correlation with any of the variables. However, the correlations of  $Y_{M/SB}$  present high degrees, indicating a high dependence of this parameter from  $x_{XP}$  and TCOD fluctuation.

### 3.3. Model generalization

Taking into account the information gathered in Sections 3.1 and 3.2, a generalized model able to predict the degradation behavior for a wide range of varying feed was developed.

**Table 4 – Correlation matrix: parameters versus organic fractions.**

	$k_1$	$k_2$	$Y$	$Y_{M/XB}$	$Y_{M/SB}$
TCOD	−0.9233	−0.9016	−0.9116	0.1733	−0.9513
SCOD	0.0683	−0.5819	−0.6283	−0.8776	−0.5396
X <sub>B0</sub>	−0.9357	−0.8143	−0.7954	0.8010	−0.9047
X <sub>I0</sub>	0.3184	−0.0972	−0.0467	0.6276	−0.0301
S <sub>B0</sub>	0.1231	−0.5603	−0.6076	−0.9027	−0.5106
S <sub>I0</sub>	−0.6647	0.1754	0.2235	0.9874	0.04105
X <sub>P0</sub>	−0.6490	−0.4092	−0.4451	−0.2920	−0.5068
X <sub>XB</sub>	−0.8815	−0.8944	−0.8757	0.8724	−0.9521
X <sub>XI</sub>	0.6303	0.3829	0.4200	0.3151	0.4794
X <sub>SB</sub>	0.7019	0.6229	0.5827	−0.9781	0.7119
X <sub>SI</sub>	−0.0754	0.9086	0.9305	0.8810	0.8548
X <sub>XP</sub>	0.0758	0.9786	0.9709	−0.8812	0.9293

As discussed above, the anaerobic degradation of biodegradable particulate material is inhibited by its own substrate. The Andrews–Haldane equation has been applied in most cases of substrate inhibition to enzymatic reactions [21], microbial growth [24,35] or microbial degradation [36]. For this reason, its application in the degradation of particulate biodegradable material is proposed here:

$$r_1 = -\frac{k \max_1 \cdot X_B}{K_{S1} + X_B + \frac{X_B^2}{K_{I1}}} \cdot X_P \quad (7)$$

where  $k \max_1$  is the maximum specific rate constant,  $K_{S1}$  is the half life constant and  $K_{I1}$  is the inhibition constant. Equation (7) was adjusted to the experimental data using the least squares method (Origin<sup>®</sup> 8.0). The  $k \max_1$  value resulted  $8762.87 \text{ L mg}^{-1} \text{ d}^{-1}$ ,  $K_{S1}$  was  $8637.10^6 \text{ mg L}^{-1}$  and  $K_{I1}$ :  $0.369 \text{ mg L}^{-1}$  ( $R^2$  adjusted = 0.59). The high value of the half life constant value indicates a low organism-substrate affinity and the low value of the inhibition constant value indicates a strong inhibition due to substrate ( $X_B$ ).

On the degradation of biodegradable soluble material, the above analysis showed that the variables that affect the degradation rate of biodegradable soluble material in the range studied were: the TCOD (which acts as inhibitor), and the inoculum-substrate ratio, which stimulates it. For this reason the generalized model included this reaction step with a non-competitive inhibition effect by TCOD [21,23] and a positive power law relation respect to  $x_{XP}$ , maintaining its first order dependence on SB and the specificity respect to the biomass,  $X_P$ :

$$r_2 = -\frac{k \max_2 \cdot (X_{XP})^n}{K_{I2} + \text{TCOD}} \cdot S_B \cdot X_P \quad (8)$$

where  $k \max_2$  is the maximum specific rate constant,  $K_{I2}$  is the inhibition constant and  $n$  is the order which affects  $x_{XP}$ . Fig. 6 shows the fit of the surface versus TCOD and  $x_{XP}$  (Origin 8.0<sup>®</sup>  $R^2$  adjusted = 0.93). In this figure it can be observed how as the inoculum-substrate ratios increases, the specific rate predicted also increases, while higher TCOD values result in lower rates. The values obtained for the parameters were:  $n = 0.304$ ;  $k \max_2 = 0.1458 \text{ L mg}^{-1} \text{ d}^{-1}$  and  $K_{I2} = 32.15 \text{ mg L}^{-1}$ . The small value of  $K_{I2}$  indicates moderate inhibition. While the low order regarding the inoculum fraction indicates it does not have a strong influence over the process. The value of  $n$  is reasonable, since several authors have found a good fit using the half-order model for biomass [26,37]. The proposed model does not consider a maximum for this ratio because experimental data do not present it.

**Table 5 – No linear regression to Equation (6).**

P	k <sub>1</sub>			k <sub>2</sub>		
	A	n	R <sup>2</sup>	A	n	R <sup>2</sup>
TCOD	6.00 × 10 <sup>8</sup>	−3.1606	0.639	2113	−1.1626	0.903
X <sub>B</sub>	71.756	−1.5252	0.999	5.00 × 10 <sup>5</sup>	−0.2279	0.985
S <sub>B</sub>	6.00 × 10 <sup>8</sup>	2.3325	0.768	0.180	−0.9603	0.326
X <sub>XP</sub>	4.00 × 10 <sup>6</sup>	2.6148	0.092	4.00 × 10 <sup>6</sup>	1.5226	0.905

P	Y <sub>M/XB</sub>			Y <sub>M/SB</sub>		
	A	n	R <sup>2</sup>	A	n	R <sup>2</sup>
TCOD	0.062	0.0657	0.0135	6.00 × 10 <sup>7</sup>	−2.4141	0.706
X <sub>B</sub>	0.035	0.1526	0.4877	1373	−0.4425	0.674
S <sub>B</sub>	3867	−0.4425	0.8697	132.7	−0.9285	0.059
X <sub>XP</sub>	0.960	−1.0896	0.8144	2.00 × 10 <sup>4</sup>	2.7941	0.553

The contribution to methane production from both degradative pathways was also considered for the generalized model. Y<sub>M/XB</sub> was considered constant and equal to the average of the observed data while Y<sub>M/SB</sub> was affected by X<sub>P</sub> and TCOD. The inhibitory effect of the total organic load (TCOD) was taken into account by a non-competitive inhibition kinetics [21] as in the previous case. However, the effect of the concentration of biomass (X<sub>P</sub>), was taken into account using a maintenance coefficient [38]. As bacterial populations growth and get old the amount of substrate required for maintenance increases, reducing the availability of nutrients for growth and generate products, what is reflected on their yield coefficients [34]. Then, the equation that describes the evolution of the methane yield coefficient due to degradation of biodegradable soluble material (Y<sub>M/SB</sub>) becomes:

$$Y_{M/SB} = \frac{Y \max_M}{K_{IM} + TCOD} - m \cdot X_P \tag{9}$$

where Ymax<sub>M</sub> is the maximum yield coefficient, K<sub>IM</sub> is the inhibition constant and m is the biomass maintenance coefficient. Fig. 7 shows the fit of the experimental surface versus TCOD and X<sub>P</sub> (Origin 8.0<sup>®</sup> R<sup>2</sup><sub>adjusted</sub> = 0.97). In this figure it is observed that lower Y<sub>M/SB</sub> values are predicted as the concentration of biomass increases according to the experimental observations. Furthermore TCOD higher values result in lower yield coefficients due to inhibition. The values obtained for the parameters were: Ymax<sub>M</sub> = 441.586 L.mg<sup>−1</sup>, K<sub>IM</sub> = 914.12 mg L<sup>−1</sup> and m = 2.79 × 10<sup>−5</sup> L.mg<sup>−1</sup>. The value of the inhibition constant indicates a substantial inhibition of

the methane yield due to total organic load, while a low maintenance coefficient indicates a slightly dependence between Y<sub>M/SB</sub> and cell maintenance.

To solve the generalized model Equations (7)–(9) were replaced in Equations (1)–(5), resulting in:

$$\frac{dX_B}{dt} = r_1 = -\frac{k \max_1 \cdot X_B}{K_{S1} + X_B + \frac{X_B^2}{K_{I1}}} \cdot X_P \tag{10}$$

$$\begin{aligned} \frac{dS_B}{dt} &= Y_H \cdot (-r_1) + r_2 \\ &= Y_H \cdot \frac{k \max_1 \cdot X_B}{K_{S1} + X_B + \frac{X_B^2}{K_{I1}}} \cdot X_P - \frac{k \max_2 \cdot (X_{XP})^n}{K_{I2} + TCOD} \cdot S_B \cdot X_P \end{aligned} \tag{11}$$

$$\frac{dX_P}{dt} = Y_{XP/SB} \cdot (r_2) = Y_{XP/SB} \cdot \frac{k \max_2 \cdot (X_{XP})^n}{K_{I2} + TCOD} \cdot S_B \cdot X_P \tag{12}$$

$$\begin{aligned} \frac{dM}{dt} &= Y_{M/XB} \cdot (-r_1) + Y_{M/SB}(TCOD, X_P) \cdot (-r_2) \\ &= Y_{M/XB} \cdot \frac{k \max_1 \cdot X_B}{K_{S1} + X_B + \frac{X_B^2}{K_{I1}}} \cdot X_P + \left( \frac{Y \max_M}{K_{IM} + TCOD} - m \cdot X_P \right) \\ &\quad \times \frac{k \max_2 \cdot (X_{XP})^n}{K_{I2} + TCOD} \cdot S_B \cdot X_P \end{aligned} \tag{13}$$

The ordinary differential equations system (10)–(13) was solved using a 4th Order Runge–Kutta routine. The predicted values are shown as solid lines in Figs. 2–5. In these figures it can be seen how the model satisfactorily predicts the behavior

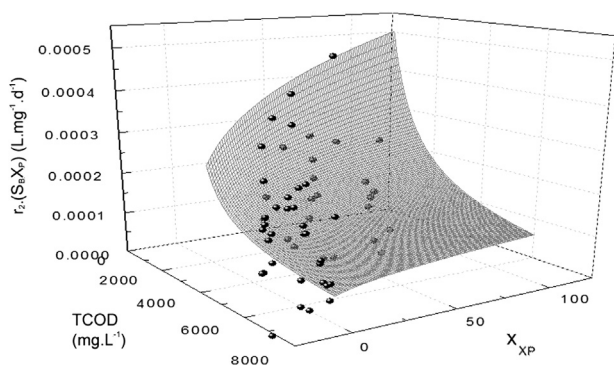


**Fig. 6 – Surface fit of Equation (8) to experimental data.**

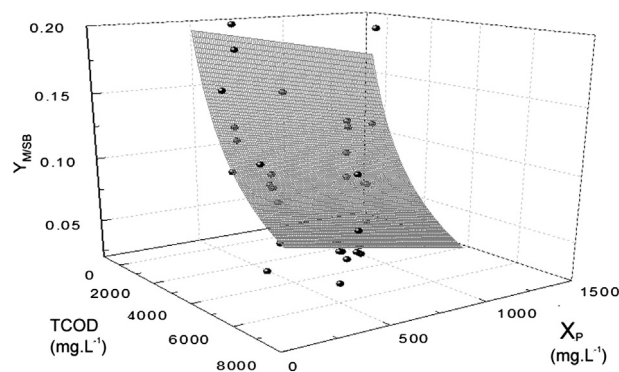


**Fig. 7 – Surface fit of Equation (9) to experimental data.**



of the all components throughout the whole process. This is more evident at long times where the previous model [7] showed some weakness of fit. In particular, it is relevant the goodness of fit for the degradation of biodegradable soluble material, a critical step of the process. Additionally, the proposed model can successfully predict the behavior of the different compounds for a wide range of feed values.

The generalized model developed in the present work represents a significant improvement with respect to the previously proposed one. From a phenomenological point of view, it considers substrate inhibition in the hydrolysis stage and non-competitive inhibition by total organic load in the step of degradation of biodegradable soluble material and the methane yield. It also takes into account the effect of biomass concentration in those stages. From the operational point of view, the model was able to successfully predict the methane production and the course of the different species in the whole concentration range studied with a single set of parameters.

#### 4. Conclusions

The variable that most affects the process as a whole is the total organic load while the biodegradable particulate organic fraction affects adversely the hydrolysis step. The information obtained allowed to develop a generalized model that considers these effects. This generalized model has been able to predict successfully the behavior of the different species throughout the whole range of conditions studied with single set of parameters. This is important in actual cases where substrates used to generate energy came from several sources and its composition could vary. Thus the model presented here demonstrated to be able to predict the performance of the process as a whole after fluctuations in the feed and it represents a considerable improvement over the previous proposed model.

#### Acknowledgments

The support was provided by grants from the National University of Mar del Plata (15/G305) and the ANPCyT (PICT N 00556). I. Durruty and N.E. Zaritzky are associated to CONICET, Argentina.

#### REFERENCES

- [1] Olthof M, Oleszkiewicz J. Anaerobic treatment of industrial wastewater. *Chem Eng* 1982;15:1321–6.
- [2] Gerardi MH. *The microbiology of anaerobic digesters*. New Jersey: John Wiley and Sons; 2003.
- [3] Chan YJ, Chong MF, Law CL, Hassell DG. A review on anaerobic-aerobic treatment of industrial and municipal wastewater. *Chem Eng J* 2009;155(1–2):1–18.
- [4] Fang C, Boe K, Angelidaki I. Biogas production from potato-juice, a by-product from potato-starch processing, in upflow anaerobic sludge blanket (UASB) and expanded granular sludge bed (EGSB) reactors. *Bioresour Technol* 2011;102(10):5734–41.
- [5] Sentürk E, Ince M, Onkal Engin G. Treatment efficiency and VFA composition of a thermophilic anaerobic contact reactor treating food industry wastewater. *J Hazard Mater* 2009;176(1–3):843–8.
- [6] Donoso-Bravo A, Mailier J, Martin C, Rodríguez J, Aceves-Lara CA, Wouwer AV. Model selection, identification and validation in anaerobic digestion: a review. *Water Res* 2011;45(17):5347–64.
- [7] Durruty I, Zaritzky NE, González JF. Kinetic studies on the anaerobic degradation of soluble and particulate matter in potato wastewater. *Biosyst Eng* 2012;111(2):195–205.
- [8] Orhon D, Artan N, Ate E. A description of three methods for the determination of the initial inert particulate chemical oxygen demand of wastewater. *J Chem Technol Biotechnol* 1994;61(1):73–80.
- [9] Neves L, Gonçalves E, Oliveira R, Alves MM. Influence of composition on the biomethanation potential of restaurant waste at mesophilic temperatures. *Waste Manag* 2008;28:965–72.
- [10] Siles JA, Martín MA, Chica A, Borja R. Kinetic modelling of the anaerobic digestion of wastewater derived from the pressing of orange rind produced in orange juice manufacturing. *Chem Eng J* 2008;140(1–3):145–56.
- [11] Vavilin VA, Fernandez B, Palatsi J, Flotats X. Hydrolysis kinetics in anaerobic degradation of particulate organic material: an overview. *Waste Manag* 2008;28(6):939–51.
- [12] Parawira W, Murto M, Zvauya R, Mattiasson B. Anaerobic batch digestion of solid potato waste alone and in combination with sugar beet leaves. *Renew Energ* 2004;29:1811–23.
- [13] Linke B. Kinetic study of thermophilic anaerobic digestion of solid wastes from potato processing. *Biomass Bioenerg* 2006;30(10):892–6.
- [14] Feng H, Hu L, Mahmood Q, Fang C, Qiu C, Shen D. Effects of temperature and feed strength on a carrier anaerobic baffled reactor treating dilute wastewater. *Desalination* 2009;239(1–3):111–21.
- [15] Fang HHP, Yu H. Mesophilic acidification of gelatinaceous wastewater. *J Biotechnol* 2002;93(2):99–108.
- [16] Raposo F, De la Rubia MA, Fernández-Cegrí V, Borja R. Anaerobic digestion of solid organic substrates in batch mode: an overview relating to methane yields and experimental procedures. *Renew Sustainable Energy Rev* 2011;16(1):861–77.
- [17] Tomei MC, Braguglia CM, Mininni G. Anaerobic degradation kinetics of particulate organic matter in untreated and sonicated sewage sludge: role of the inoculum. *Bioresour Technol* 2008;99:6119–26.
- [18] Angenent LT, Abel SJ, Sung S. Effect of an organic shock load on the stability of an anaerobic migrating blanket reactor. *J Environ Eng* 2002;128:1109–20.
- [19] Stanchev V, Stoilova I, Krastanov A. Biodegradation dynamics of high catechol concentrations by *Aspergillus awamori*. *J Hazard Mater* 2008;154(1–3):396–402.
- [20] Batstone DJ, Keller J, Angelidaki I, Kalyuzhnyi SV, Pavlostathis SG, Rozzi A, et al. The IWA anaerobic digestion model No 1 (ADM1). *Water Sci Technol* 2002;45(10):65–73.
- [21] Blanch HW, Clark DS. *Biochemical engineering*. New York: Marcel Dekker Inc.; 1996.
- [22] Wolski E, Durruty I, Haure P, González J. *Penicillium chrysogenum*: phenol degradation abilities and kinetic model. *Water Air Soil Pollut* 2012;223(5):2323–32.
- [23] Mösche M, Jördening H-J. Comparison of different models of substrate and product inhibition in anaerobic digestion. *Water Res* 1999;33(11):2545–54.

- [24] Bhunia P, Ghangrekar MM. Analysis, evaluation, and optimization of kinetic parameters for performance appraisal and design of UASB reactors. *Bioresour Technol* 2008;99(7):2132–40.
- [25] Kus F, Wiesmann U. Degradation kinetics of acetate and propionate by immobilized anaerobic mixed cultures. *Water Res* 1995;29(6):1437–43.
- [26] Saravanane R, Murthy DVS, Krishnaiah K. Anaerobic fluidized bed degradation and the development of a kinetic model for a particulate organic matter enriched wastewater sludge. *Water Air Soil Pollut* 2001;127(1):15–30.
- [27] APHA. Standard methods for the examination of water and wastewater. 20th ed. Washington DC, USA: American Public Health Association/American Water Works Association/Water Environment Federation; 1998.
- [28] Eiroa M, Costa JC, Alves MM, Kennes C, Veiga MC. Evaluation of the biomethane potential of solid fish waste. *Waste Manag* 2012;32(7):1347–52.
- [29] McCarty PL. Anaerobic waste treatment fundamentals – chemistry and microbiology. *Public Works* 1964;95:107.
- [30] Yang X, Lauzon CB, Crainiceanu C, Caffo B, Resnick SM, Landman BA. Biological parametric mapping accounting for random regressors with regression calibration and model II regression. *NeuroImage* 2012;62(3):1761–8.
- [31] Gunaseelan VN. Regression models of ultimate methane yields of fruits and vegetable solid wastes, sorghum and napiergrass on chemical composition. *Bioresour Technol* 2007;98(6):1270–7.
- [32] Moreno-Andrade I, Buitrón G. Influence of the initial substrate to microorganisms concentration ratio on the methanogenic inhibition. *Water Sci Technol* 2003;48(6):17–22.
- [33] Durruty I, Okada E, González JF, Murialdo S. Degradation of chlorophenol mixtures in a fed-batch system by two soil bacteria. *Water SA* 2011;37(4):547–52.
- [34] van Bodegom P. Microbial maintenance: a critical review on its quantification. *Microb Ecol* 2007;53(4):513–23.
- [35] Bajaj M, Gallert C, Winter J. Phenol degradation kinetics of an aerobic mixed culture. *Biochem Eng J* 2009;46(2):205–9.
- [36] Agarry SE, Solomon BO, Layokun SK. Kinetics of batch microbial degradation of phenols by indigenous binary mixed culture of *Pseudomonas aeruginosa* and *Pseudomonas fluorescens*. *Afr J Biotechnol* 2008;7(14):2417–23.
- [37] Münch Ev, Keller J, Lant P, Newell R. Mathematical modelling of prefermenters-I. Model development and verification. *Water Res* 1999;33(12):2757–68.
- [38] Pirt SJ. Principles of microbial and cell cultivation. Oxford: Blackwell Scientific, Publications; 1975.